Light transport in one-dimensional arrays of infinitesimal magnetoactive dielectric sheets: Theory and numerical simulations

Vladimir Gasparian,[1] Zhyrair Gevorkian,[2,3,*] and Oscar del Barco[4]
[1]*California State University, Bakersfield, California, USA*
[2]*Yerevan Physics Institute, Alikhanian Brothers St. 2, 0036 Yerevan, Armenia*
[3]*Institute of Radiophysics and Electronics, Ashtarak-2, 0203, Armenia*
[4]*Departamento de Física - CIOyN, Universidad de Murcia, Murcia, Spain*
(Received 3 July 2013; published 23 August 2013)

We have provided a complete description of light propagation at an oblique angle of incidence in disordered one-dimensional (1D) ultrathin magnetophotonic crystals with an arbitrary number of sheets. We have shown that in the long-wavelength limit, when the parameter $\frac{d\epsilon_{L,R}}{\lambda}$ is much less than unity ($\epsilon_{L,R}$ is the relative permittivity for left- and right-polarized light, d is the thickness of the sheet, and λ is the wavelength), the photon transport problem in a 1D magnetophotonic crystal is identical to Anderson's two-channel model. In our discussion we include mode conversion and derive exact and closed analytical expressions for all scattering matrix elements. We have calculated the Faraday and Kerr rotational angles for a periodic system. Our formulas predict correctly the main trends of magneto-optic effects in 1D systems. We also derived analytical expressions for photon localization lengths, in a weak disordered regime, for s and p modes and for circular polarized light. We demonstrate that the presence of coupling modes enhances ξ_s and reduces ξ_p with respect to the values $\xi_s(0)$ and $\xi_p(0)$ obtained when the coupling modes are absent. Presented analytical expressions for localization lengths are in good agreement with numerical calculations, exact up to order δ^2 (δ being the disorder strength), and valid up to angles of incidence of 1.56 rad.

DOI: 10.1103/PhysRevA.88.023842 PACS number(s): 42.25.Dd, 73.20.Fz, 41.75.Jv

I. INTRODUCTION

One-dimensional magnetophotonic crystals (1D MPCs) are very attractive systems not only for practical applications [1–4], but also for theoretical and numerical studies [5–16]. The advantage of 1D systems is that they can be solved analytically within some approximations. The behavior of electromagnetic waves (EMWs) in magnetic multilayers (mostly with periodic profile) has been studied [5–16]. In Refs. [5,6], using a transfer matrix method, an enhancement of the magneto-optic effects at the band edges of 1D photonic crystals was found, while in Ref. [7] the authors demonstrated an alteration of the band structure in two-dimensional MPCs. The authors of Ref. [8] studied, using a general group-theoretical method, a magnetic layer sandwiched between a pair of identical periodic nonmagnetic stacks (Bragg reflectors), and periodic layered structures composed of alternate magnetic and dielectric layers. It has been shown that the band structure of photonic crystals composed of materials with natural magneto-optic activity can be modified by external static magnetic or electric fields [9,10]. Fewer papers have been devoted to propagation of EMWs in disordered MPCs [17–20]. Recently, the effect of disorder on the transmittance of MPCs has been discussed in Ref. [17] in a short-wavelength approximation, where the localization is strong. In this approximation the multipass reflections are neglected so that the total transmission coefficient is approximated by the product of the single-layer transmission coefficients.

At present, most numerical simulations are available as one of the effective tools to analyze the behavior of an electromagnetic wave in magnetic multilayer systems, without any restriction on the number of individual layers or on the angle of incidence of the optical wave. The general approach which serves as a basis for numerical and qualitative analysis of propagation of EMWs in 1D MPCs is the 4×4 transfer matrix [3]. In the framework of transfer matrices, in each MPC layer, there are four waves propagating independently of each other in two opposite directions, and any attempt to get closed analytical expressions for the reflection or transmission amplitudes in 1D MPCs with a finite number of layers, based on the 4×4 matrix approach, is practically impossible.

One reason is that the products of the individual transfer matrices do not commute, and one needs to calculate the product of all transfer matrices which exponentially increases with their number. This is the main difficulty of the transfer matrix method, which has been present in many studies of the localization length in 1D disordered systems (see, e.g., Refs. [21,22]).

Another reason is that, because of the anisotropy of the medium, mode coupling appears at the interface, and even for the special case of a periodic layered medium, closed forms for the reflection and transmission amplitudes are too complicated to derive [3].

To simplify the calculations and avoid any mode coupling in 1D MPCs, the transmission and reflection magneto-optic effects in a periodic magnetic multilayer were described using the formalism originally developed for an isotropic multilayer [11]. The simplifications are made possible thanks to the restriction to the normal light incidence and assuming the absence of mode conversion. In this particular case the product of transfer matrices M can be replaced just by a block diagonal matrix with the off-diagonal blocks being zero matrices [11]. Then, making use of the properties of Chebyshev polynomials, in Ref. [11] the analytical representations for the transfer matrix M of a periodic multilayer with arbitrary modes

*gevork@yerphi.am

were provided. However, ignoring the mode conversion is an essential simplification, and this is the main reason why the approximate expressions well reproduce the results of the exact numerical calculations in a very narrow range of magnetic film thicknesses and depend on the wavelength and polarization state of the incident radiation (see Ref. [11] for more details).

Another type of simplification of transfer matrix M in magnetic multilayer systems, which still describes the process correctly, can be reached by using the ultrathin film approximation [13–15], assuming that a layer thickness is much smaller than the radiation wavelength (in the nth layer medium). In this approach, the off-diagonal elements of the individual transfer matrix $M^{(n)}$ are different from zeros, in contrast to the model discussed in Ref. [11]. Based on Bloch's theorem and the explicit expression of a single transfer matrix $M^{(n)}$, the energy spectra of infinite periodic structures were studied in 1D and 2D systems in Refs. [13–15]; however, probably because of technical difficulties inherent to the transfer matrix method, the disordered multilayer systems were left out of their discussions.

In the present paper we develop a different approach to study the behavior of EMWs in disordered 1D PMCs, based on the ultrathin film approximation combined with the characteristic determinant (CD) method, originally introduced to study the quantum transport of electrons in quasi-one-dimensional (Q1D) disordered systems [23,24]. The CD method allows one a sufficiently complete description of electron behavior mapped into a 1D problem with modified matrix elements and without actually determining the eigenfunctions of the electron.

In our discussion we will remove the limitations on the normal incident light and on the absence of mode conversion, which was an essential assumption in Ref. [11]. We will assume that s and p modes are coupled to each other via a magnetically induced anisotropy [see below, Eq. (1)] and, we will relate the EMW propagation problem to the Anderson localization of electrons in Q1D systems with two channels. The mapping of the light propagation in a 1D PMC disordered system to quantum transport of electrons in the Q1D strip model is done in three steps. First, one introduces the conventional description of the electron's scattering matrix elements in terms of characteristic determinants. In the second step, the characteristic determinants are written in terms of individual light scattering parameters, using the equivalence of electrons and electromagnetic waves. Finally, using the scattering matrix elements (20) and (21), we properly describe the asymptotic behavior of an EMW in 1D MPCs. The last step was based on the fact that the parameter $|\gamma| \equiv \frac{4\pi^2 d^2 \epsilon_L \epsilon_R}{\lambda^2}$ is much less than unity [$\epsilon_{L,R}$ is the relative permittivity for left- and right-polarized light, d is the thickness of sheet, and λ is the wavelength; see below, Eq. (17)] in the whole range of the wavelength (approximately from 600 to 1300 nm) where the magneto-optic parameters have been studied experimentally (see, e.g., Refs. [11,12,25] and references therein).

Thus, the existence of such a small parameter γ indicates that the propagation of light in 1D MPCs and charge transport in a Q1D disordered two-channel system become equivalent. The last step will have to be justified, but the advantage of this step should be obvious: the whole theory of EMW scattering reduces to the problem of calculating the determinants. We will come back to this point below in more detail, but note that the results of our simulation support the analytical expressions based on this assumption (see Sec. V).

Thereby, throughout the paper we will assume that the inequality $|\gamma_n| \ll 1$ is satisfied for all the real parameters that characterize each of the MPC's sheets (see, e.g., Refs. [15,25]). Taking into account this condition, we will calculate the localization length of an EMW in 1D MPC systems in the weakly disordered systems for s-, p-, and circularly polarized waves. The approach will allow us to calculate analytically the scattering matrix elements for EMWs in 1D disordered MPCs without actually determining the eigenfunctions of the light. It will be shown that the elements of reflection and transmission amplitudes may be presented in the form of a ratio of two determinants where both the numerator and the denominator are polynomials of Nth degree (N is the number of MPC sheets).

The work is organized as follows. In Sec. II we formulate the problem. In Sec. III we consider the technically simple case of the periodic structure, and appropriate analytical expressions for scattering matrix elements and for Faraday and Kerr angles of rotations are derived. Disordered systems are studied in Sec. IV where we calculate the localization lengths for s and p modes, as well as for circularly polarized light. Numerical results are presented in Sec. V. They are in excellent agreement with our analytical expressions for scattering matrix elements and localization lengths. Finally, the main conclusions are summarized in Sec. VI. In the Appendix we show the explicit expressions for the transmission amplitude, $T_{ss}^{(2)}$, for the case of two different sheets calculated directly: (i) multiplying the individual transfer matrices, Eq. (1), by hand and (ii) from the determinant expression [see Eq. (21)].

II. 1D ARRAY OF N INFINITESIMAL MAGNETOACTIVE SHEETS

Let us consider a 1D array of N MPC layers with spatial period a, as shown in Fig. 1. Incident light with a wave number k enters from the left at an angle θ with respect to the x axis. We choose the plane $y0z$ coinciding with the boundary of two media, and the plane $z0x$ coinciding with the plane of the incident wave. Each slab is assumed to have vacuum on either side and has a thickness d and relative permittivities ϵ_L and ϵ_R for left- and right-polarized light, respectively. The

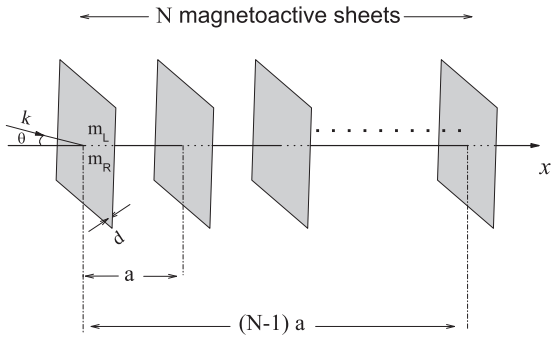

FIG. 1. A one-dimensional array of N infinitesimal magnetoactive sheets with spatial period a. Light enters from the left at an angle θ with respect to the x axis and with wave number k. Each MS is characterized by the parameters $m_L = \epsilon_L d$ and $m_R = \epsilon_R d$ where the thicknesses $d \to 0$ and the relative permittivities ϵ_L and ϵ_R tend to infinity.

general procedure to study the propagation and the Anderson localization of p- and s-polarized electromagnetic waves incident obliquely on such a 1D array of N magnetoactive sheets is to solve the wave equation for the complex amplitude of vector $\vec{E}$ (or $\vec{H}$) for the nth layer with given relative permittivity tensor $\epsilon^n_{i,j}$. Since the tangential components of the electric and magnetic fields on the boundary are continuous, one can evaluate 4×4 the dynamical matrix $M^{(n)}$, which matches electric field amplitudes from the left side of the boundary to the right side. By multiplication of the 4×4 individual transfer matrices $M^{(n)}$, we will arrive at the final matrix $M=\prod_{n=1}^{N} M^{(n)}$, which takes into account the multiple reflection and represents the given structure with the particular disorder configuration.

However, as was mentioned in the Introduction, in principle it is impossible to get the analytical exact expressions for the scattering matrix elements in a 1D disordered MPC multilayer with an arbitrary number N of slabs, based on $M=\prod_{n=1}^{N} M^{(n)}$. This must be done either numerically (see, e.g., Refs. [5,6]) or we need to find a significantly simplified algorithm which allows one to calculate the matrix M without affecting the peculiar features of MPCs. For the present purpose we develop a method based on the ultrathin film approximation [13–15] combined with the characteristic determinant method [23,24]. In the approximation of infinitesimal sheets we let the thickness d of the magneto-optic layer tend to zero, $\epsilon_L\to\infty$, and $\epsilon_R\to\infty$, in such a way that the products $\epsilon_L d=m_L=\text{const}$ and $\epsilon_R d=m_R=\text{const}$. In this limiting case the expression for the 4×4 transfer matrix of the nth single magneto-optic active layer, which relates the electric and magnetic fields of incident light on the left and right sides, can be written as [3,15]

$$M^{(n)}=\begin{pmatrix} 1+ix_n & +ix_n & z_n & z_n \\ -ix_n & 1-ix_n & -z_n & -z_n \\ -z_n & -z_n & 1+iy_n & +iy_n \\ z_n & z_n & -iy_n & 1-iy_n \end{pmatrix}, \tag{1}$$

where k and k_x are defined in the optically inactive medium. The rest of the parameters are defined as follows: $x_n=\frac{m_n}{2}\frac{k^2}{k_x}$; $y_n=\frac{m_n}{2}k_x$; $z_n=\Delta_n\frac{k}{4}$; $2m_n=(m_L)_n+(m_R)_n=\text{const}$; $\Delta_n=(m_L)_n-(m_R)_n=\text{const}$. The latter two parameters with dimensions of length, m_n and Δ_n, are the averaged optical property and its magnetically induced anisotropy of a single nth sheet [11] and characterize the 1D MPC system in the limit of infinitesimal thickness. The inhomogeneous dielectric tensor $\epsilon_{i,j}$ varies only in the x direction: it is unity everywhere except the planes that are located at $x=na$ $[n=0,1,\ldots,(N-1)]$. From Eq. (1) it follows, as one must expect, that if the parameter of magneto-optic activity Δ is equal to zero, then the transfer matrix $M^{(n)}$ reduces to a block diagonal matrix and one can separate s and p polarizations. If Δ is not equal to zero, then we are dealing with the hybrid mode and a simple separation of s and p modes becomes impossible. In the sense of coupling modes a 1D MPC is similar in spirit to two different models for a disordered quasi-one-dimensional wire where the coupling constant mixes all the modes and the Shrödinger equation for a discrete lattice becomes a set of infinitely coupled algebraic equations [26,27]. The models are (i) a set of N two-dimensional Dirac δ potentials V_l with signs and strengths determined randomly: $V(x,y)=\sum_{l=1}^{N} V_l\delta(x-x_l)\delta(y-y_l)$; and (ii) a Q1D disordered lattice of size $N\times M$ described by the standard tight-binding Hamiltonian with modes M and on-site disorder: $H=\sum_{j=1}^{N}\sum_{l=1}^{M}|j,l\rangle\epsilon_{j,l}\langle j,l|-t\sum_{j,l}\sum_{\delta=\pm1}\{|j,l\rangle\langle j+\delta,l|+|j,l\rangle\langle j,l+\delta|\}$ ($\epsilon_{j,l}$ is the strength of the random potential at site (j,l) and t is the hopping matrix element). The Dyson equation for the two models was solved exactly, without any restriction on the numbers of impurities (N) and modes (M) [23,24]. The CD approach leads to the description of the scattering matrix elements in terms of determinants of rank $N\times N$ that are built up of the transmission and reflection coefficients of the individual scatterer.

We shall not repeat here the calculations presented in Refs. [23,24], but state the final expressions for an electron's scattering elements in an M multichannel system. For reflection $R^{(N)}_{nm}$ and transmission $T^{(N)}_{nm}$ amplitudes for an electron, incident from the left, we have

$$R^{(N)}_{nm}=(-1)^N\frac{1}{\det\left(D^{(N)}_{i,j}\right)_1}\times\begin{vmatrix} 0 & r^{(1)}_{nm} & \cdots & r^{(N)}_{nm}e^{ik_{xn}|x_N-x_1|} \\ 1 & \cdots & \cdots & \cdots \\ \vdots & \vdots & & \left(D^{(N)}_{i,j}\right)_m \\ e^{ik_{xm}|x_N-x_1|} & \vdots & & \end{vmatrix} \tag{2}$$

and

$$T^{(N)}_{nm}=(-1)^N\frac{e^{ik_{xm}(x_N-x_1)}}{\det\left(D^{(N)}_{i,j}\right)_1}\times\begin{vmatrix} \delta_{nm} & r^{(1)}_{nm} & \cdots & r^{(N)}_{nm}e^{ik_{xn}|x_N-x_1|} \\ 1 & \cdots & \cdots & \cdots \\ \vdots & \vdots & & \left(D^{(N)}_{i,j}\right)_m \\ e^{-ik_{xm}|x_N-x_1|} & \vdots & & \end{vmatrix}, \tag{3}$$

respectively. The index n (m) indicates the nth (mth) channel. k_{xn} is the wave vector in the nth channel and is defined as ($\hbar=2m_0=1$)

$$k_{xn}=+\sqrt{E-\frac{n^2\pi^2}{W^2}} \tag{4}$$

for the two-dimensional Dirac δ potentials with hard wall conditions in the y direction (E is the Fermi energy, n is the subband index, and W is the width of the system in the y direction). For the TB model k_{xn} is defined as

$$E=\begin{cases} 2t\cos k_{xn}+2t\cos\frac{\pi n}{M+1}, & n=1,2,\ldots,M, \text{ hard wall conditions,} \\ 2t\cos k_{xn}+2t\cos\frac{2\pi n}{M}, & n=0,1,\ldots,M-1, \text{ periodic boundary conditions.} \end{cases} \tag{5}$$

If the electron is incident along the mth channel, then $r_{nm}^{(l)}$ is the reflection amplitude from the nth channel for the isolated potential V_l (or $\epsilon_{j,l}$) in the absence of the remaining $(N-1)$ potentials [23,24,27]. The numerators of $R_{nm}^{(N)}$ and $T_{nm}^{(N)}$ are obtained from the quantity $\det(D_{i,j}^{(N)})_m$ by augmenting it on the left and on the top. The matrix elements of the denominator $(D_{i,j}^{(N)})_m$, which contains information about the number of modes M $[1 \leqslant i,j \leqslant N;\ 1 \leqslant m \leqslant M]$, are

$$\left(D_{i,j}^{(N)}\right)_m = -\delta_{ij} + (1-\delta_{ij}) \sum_{p=1}^{M} \frac{r_{1p}^{(i)} r_{pm}^{(j)}}{r_{1m}^{(i)}} e^{ik_p|x_j - x_i|}. \tag{6}$$

Notice that, for both mentioned models, $r_{nm}^{(l)}$ satisfies the condition

$$r_{mm}^{(l)} r_{nn}^{(l)} - r_{mn}^{(l)} r_{nm}^{(l)} = 0 \tag{7}$$

and is completely independent of the boundary conditions (see Refs. [23,24,27]).

As we will see below, this condition plays a key role in this study and allows one to map the problem of the EMW propagation in 1D MPCs onto a Q1D strip model with two channels, assuming that the same type of condition is also true for the photon's reflection amplitudes from a single sheet.

Therefore, before considering the full set of N MPC sheets presented in Fig. 1, it is worth verifying the relation (7). To this end, let us first study a single sheet and find the transmission and reflection amplitudes for s and p modes. Let us define the electric field transmission and reflection amplitudes for s modes (with electric field vector $\vec{E}$ perpendicular to the plane of incidence) in the matrix form

$$\begin{pmatrix} t_{ss}^{(n)} \\ 0 \\ t_{sp}^{(n)} \\ 0 \end{pmatrix} = M^{(n)} \begin{pmatrix} 1 \\ r_{ss}^{(n)} \\ 0 \\ r_{sp}^{(n)} \end{pmatrix}, \tag{8}$$

where $M^{(n)}$ is given by (1).

The physical meaning of the scattering matrix elements $t_{nm}^{(n)}$ and $r_{nm}^{(n)}$ $(n,m = s,p)$ is clear: $t_{nm}^{(n)}$ is the transmission amplitude of the light through the single sheet from the channel n to the channel m, $r_{nm}^{(n)}$ is the reflection amplitude from the nth channel, if the photon is incident along the mth channel. The transmission, $t_{nm}^{(n)}$, and reflection, $r_{nm}^{(n)}$, amplitudes are expressed in terms of matrix elements of $M^{(n)}$ as follows:

$$t_{ss}^{(n)} = \frac{1 - iy_n}{A_n}, \tag{9}$$

$$t_{sp}^{(n)} = -\frac{z_n}{A_n}, \tag{10}$$

$$r_{ss}^{(n)} = \frac{ix_n - \gamma_n}{A_n}, \tag{11}$$

$$r_{sp}^{(n)} = -\frac{z_n}{A_n}, \tag{12}$$

where

$$A_n = 1 - ix_n - iy_n + \gamma_n$$

with $\gamma_n \equiv z_n^2 - x_n y_n = -4\pi^2 (m_L)_n (m_R)_n / \lambda^2$. In a similar way we calculate the parameters $t_{pp}^{(n)}$, $t_{ps}^{(n)}$, $r_{pp}^{(n)}$, and $r_{ps}^{(n)}$ for p-polarized light, when the electric vector $\vec{E}$ lies in the plane of incidence:

$$t_{pp}^{(n)} = \frac{1 - ix_n}{A_n}, \tag{13}$$

$$t_{ps}^{(n)} = \frac{z_n}{A_n}, \tag{14}$$

$$r_{pp}^{(n)} = \frac{iy_n - \gamma_n}{A_n}, \tag{15}$$

$$r_{ps}^{(n)} = \frac{z_n}{A_n}. \tag{16}$$

It is easy to check that the conservation law takes effect for s (p) waves:

$$t_{ss}^{(n)} t_{ss}^{(n)*} + r_{ss}^{(n)} r_{ss}^{(n)*} + t_{sp}^{(n)} t_{sp}^{(n)*} + r_{sp} r_{sp}^{(n)*} = 1.$$

As for the condition (7), we have

$$r_{ss}^{(n)} r_{pp}^{(n)} - r_{sp}^{(n)} r_{ps}^{(n)} = \frac{\gamma_n}{A_n}. \tag{17}$$

One can see that, in contrast to the case of tight-binding and delta potential models [see Eq. (7)], the right-hand side of the above equation is not zero. However, as it was mentioned above, in the long-wavelength approximation the parameter $|\gamma_n|$ is very small. Hence, in this approximation the right-hand side of Eq. (17) will be replaced by zero and will justify the application of the CD formalism to the propagation of EMWs in 1D MPC disordered systems. It is important to note that the condition $|\frac{\gamma_n}{A_n}| \ll 1$ does not lead to ignoring the coupling of s and p modes. As we will see later (see Sec. V), in the relatively large wavelength limit where most of the experiments were done, the mentioned inequality is satisfied (see for example Refs. [5,6,15,25]).

Keeping in mind the mentioned inequality, the denominator of (2) and (3), for s and p modes, can be rewritten as

$$\left(D_{i,j}^{(N)}\right)_s = -\delta_{ij} + (1-\delta_{ij}) \left[r_{ss}^{(j)} + \frac{r_{sp}^{(i)} r_{ps}^{(j)}}{r_{ss}^{(i)}} \right] e^{ik_x|x_j - x_i|}. \tag{18}$$

Naturally, the scattering matrix elements (2) and (3) can alternatively be calculated using also the following denominator:

$$\left(D_{i,j}^{(N)}\right)_p = -\delta_{ij} + (1-\delta_{ij}) \left[r_{pp}^{(j)} + \frac{r_{ss}^{(i)} r_{sp}^{(j)}}{r_{sp}^{(i)}} \right] e^{ik_x|x_j - x_i|}. \tag{19}$$

The final answer for scattering matrix elements is insensitive to these changes. We remind the reader that in Eqs. (18) and (19) $r_{nm}^{(j)}$ $(n,m = s,p)$ are reflection amplitudes from a single sheet and are given by Eqs. (11), (12), (15), and (16).

The final expressions for the total reflection and transmission amplitudes $R_{nm}^{(N)}$ and $T_{nm}^{(N)}$ $(n,m = s,p)$ which we are going to use throughout the paper are

$$R_{nm}^{(N)} = (-1)^N \frac{1}{\det\left(D_{i,j}^{(N)}\right)_s} \times \begin{vmatrix} 0 & r_{nm}^{(1)} & \cdots & r_{nm}^{(N)} e^{ik_x|x_N - x_1|} \\ 1 & \cdots & \cdots & \cdots \\ \vdots & \vdots & & (D_{i,j}^{(N)})_s \\ e^{ik_x|x_N - x_1|} & \vdots & & \end{vmatrix}, \tag{20}$$

$$T_{nm}^{(N)} = (-1)^N \frac{e^{ik_x(x_N - x_1)}}{\det\left(D_{i,j}^{(N)}\right)_s} \times \begin{vmatrix} \delta_{nm} & r_{nm}^{(1)} & \cdots & r_{nm}^{(N)} e^{ik_x|x_N - x_1|} \\ 1 & \cdots & \cdots & \cdots \\ \vdots & \vdots & & (D_{i,j}^{(N)})_s \\ e^{-ik_x|x_N - x_1|} & \vdots & & \end{vmatrix}. \quad (21)$$

We would like to recall that the photon's scattering matrix elements (20) and (21) are exact, valid for an arbitrary disordered profile without any restriction on the number of sheets, provided that $|\gamma_n| \ll 1$.

Modeling of the optical response of a 1D MPC disordered system in terms of the proposed characteristic determinant formalism has a few advantages: First, for a small number of sheets the determinant can be calculated easily (see the Appendix). Second, the addition of one MPC sheet in the system with N sheets corresponds to the addition of one new row and new column in $D^{(N)}$. This means that in some particular cases (e.g., periodic and quasiperiodic structures) one can write a recurrence relationship for a determinant $D^{(N)}$ (see Sec. III). Finally, using the general method of expanding a determinant in terms of its complementary minors in the weak disorder regime, one can calculate the localization lengths for s and p modes (see Sec. IV).

III. PERIODIC SYSTEM

Unfortunately, there is no technique for calculating the scattering matrix elements, Eqs. (20) and (21), in the general case of N disordered sheets (one needs to evaluate large $N \times N$ matrices with arbitrary elements). However, the periodic structure, due to its simplicity, enables us to resolve the problem and get closed analytical expressions for scattering matrix elements. This will be done in this section. In the next section ("Disordered system") we calculate the localization lengths based on the approximate expressions (45) and (46).

First, let us evaluate the denominator of expressions (20) and (21). After tedious but straightforward calculations one can show that the determinant D_N, Eq. (18) [or (19)] can be presented in tridiagonal Toeplitz form, where the only nonzero elements are the diagonal elements nn, and the nearest-neighbor elements $n \pm 1$. Hence, determinant D_N satisfies the following recurrence relationship:

$$D_N = 2e^{ik_x a} \cos\beta a\, D_{N-1} - e^{2ik_x a} D_{N-2}, \quad (22)$$

where D_{N-1} (D_{N-2}) is the determinant in the form (18) with the Nth [and also the $(N-1)$th] row and column omitted. The initial conditions in the previous recurrence relations are

$$D_{-1} = 0, \quad D_0 = 1, \quad D_1 \equiv A_1 = 1 - i\frac{m\left(k^2 + k_x^2\right)}{2k_x}. \quad (23)$$

Here β plays the role of quasimomentum and is defined by the dispersion relation

$$\cos\beta a = \mathrm{Re}\left\{e^{-ik_x a}\left(1 - i\frac{m\left(k^2 + k_x^2\right)}{2k_x}\right)\right\} = \cos k_x a - \frac{m\left(k^2 + k_x^2\right)}{2k_x}\sin k_x a. \quad (24)$$

This transcendental equation for the photonic band structure for a 1D MPC is analogous to the solution of the Kronig-Penney model in the electronic structure problem, provided that the inequality $|\gamma/A| \ll 1$ takes place in the periodic system. When the modulus of the right-hand side of Eq. (24) turns out to be greater than 1, β has to be taken as imaginary. This situation corresponds to a forbidden gap in the frequency spectrum of an infinite system. It is worth noting that Eq. (24) does not coincide with the expression expected from the exact dispersion relation [15], based on an expansion over a small parameter of the magnetically induced anisotropy Δ [see Eq. (1)]. Equation (24) mixes the two modes channels, and thereby can serve as the dispersion relation for both p and s modes simultaneously.

To find a solution of Eq. (22), note that D_N can be presented in the form $D_N = c_1 U_1^N + c_2 U_2^N$, where U_1 and U_2 are the solutions of the equation

$$U^2 - 2e^{ik_x a}\cos\beta a\, U + e^{2ik_x a} = 0. \quad (25)$$

c_1 and c_2 are assumed to satisfy the initial conditions $D_0 = c_1 + c_2 = 1$ and $D_1 = c_1 U_1 + c_2 U_2 = 1 - i\frac{m(k^2+k_x^2)}{2k_x}$. Solving Eq. (25) and taking into account the initial conditions for c_1 and c_2, we obtain for D_N the following expression:

$$D_N = e^{iNk_x a}\left\{\cos N\beta a + i\,\mathrm{Im}\left[e^{-ik_x a}\left(1 - i\frac{m\left(k^2 + k_x^2\right)}{2k_x}\right)\right]\frac{\sin N\beta a}{\sin\beta a}\right\}. \quad (26)$$

Expression (26) indicates that the denominator of scattering matrix elements D_N is $(-1)^l e^{iNk_x a}$, for all N when the interference term $\sin N\beta a/\sin\beta a = 0$. The former occurs at $N\beta a = \pi l$ and produces $N-1$ oscillations in each spectral band associated with the total system length Na. Note that above described behavior of D_N is similar to the one obtained in 1D periodic systems with nonmagnetic sheets (see for example, Refs. [28,29]).

A. Scattering matrix elements

1. *s polarization*

As mentioned, the numerator of $T_{nm}^{(N)}$, Eq. (21), is obtained from the same determinant (19) by augmenting it on the left and on the top. This fact and the periodicity enables us to calculate the numerator of $T_{ss}^{(N)}$. Presenting the latter as a determinant of a tridiagonal matrix and using similar recurrence relations found for D_N [see Eq. (22)], one can get for the numerator a closed solution in the form $\frac{k_x^2}{k^2+k_x^2}(D_N + \frac{k^2}{k_x^2})$. Hence

$$T_{ss}^{(N)} = e^{ik_x(N-1)a}\frac{k_x^2}{k^2 + k_x^2}\left(D_N + \frac{k^2}{k_x^2}\right)D_N^{-1}. \quad (27)$$

In a similar way one can show that

$$T_{sp}^{(N)} = -ie^{ik_x(N-1)a}\frac{k_x k}{k^2 + k_x^2}\frac{\Delta}{2m}(D_N - 1)D_N^{-1}, \quad (28)$$

$$R_{ss}^{(N)} = -im\frac{k^2}{2k_x}\frac{\sin N\beta a}{\sin\beta a}e^{i(N-1)k_x a}\frac{1}{D_N}, \quad (29)$$

and finally

$$R_{sp}^{(N)} = \Delta \frac{k}{4} \frac{\sin N\beta a}{\sin \beta a} e^{i(N-1)k_x a} \frac{1}{D_N}. \tag{30}$$

2. *p polarization*

The numerator of $T_{pp}^{(N)}$ can be found in a similar way. Hence, the final answers for scattering matrix elements for p modes are

$$T_{pp}^{(N)} = e^{ik_x(N-1)a} \frac{k^2}{k^2 + k_x^2} \left(D_N + \frac{k_x^2}{k^2} \right) \frac{1}{D_N}, \tag{31}$$

$$R_{pp}^{(N)} = -im \frac{k_x}{2} \frac{\sin N\beta a}{\sin \beta a} e^{i(N-1)k_x a} \frac{1}{D_N}, \tag{32}$$

$$T_{ps}^{(N)} = -T_{sp}^{N}, \tag{33}$$

$$R_{ps}^{(N)} = -R_{sp}^{N}. \tag{34}$$

B. Conservation law

Via Eqs. (27)–(30) it is straightforward to check that, for the scattering matrix elements of s modes, intensity conservation takes place:

$$\left|T_{ss}^{(N)}\right|^2 + \left|T_{sp}^{(N)}\right|^2 + \left|R_{ss}^{(N)}\right|^2 + \left|R_{sp}^{(N)}\right|^2 = 1 - \frac{8m_L m_R}{(m_L + m_R)^2} \frac{k_x^2 k^2}{\left(k_x^2 + k^2\right)^2} \left(1 - \frac{\mathrm{Re}\, D_N}{|D_N|^2} \right), \tag{35}$$

with

$$|D_N|^2 = D_N D_N^* = \left[1 + \left(\frac{m\left(k^2 + k_x^2\right)}{2k_x} \right)^2 \frac{\sin^2 N\beta a}{\sin^2 \beta a} \right]. \tag{36}$$

Expression (35) is practically equal to 1 for a wide range of parameters. A similar equation holds for the p modes.

C. Magneto-optic effects

For an incident wave linearly polarized parallel to the y axis the expressions for Faraday and Kerr rotational angles are as follows.

(1) s polarization:

$$\tan \theta_s^T = -\frac{T_{sp}^{(N)}}{T_{ss}^{(N)}} = i \frac{k}{k_x} \frac{(m_L - m_R)(D_N - 1)}{(m_L + m_R)\left(D_N + \frac{k^2}{k_x^2}\right)}, \tag{37}$$

$$\tan \theta_s^R = -\frac{R_{sp}^{(N)}}{R_{ss}^{(N)}} = i \frac{k_x}{k} \frac{m_L - m_R}{m_L + m_R}. \tag{38}$$

(2) p polarization:

$$\tan \theta_p^T = -\frac{T_{ps}^{(N)}}{T_{pp}^{(N)}} = -i \frac{k_x}{k} \frac{(m_L - m_R)(D_N - 1)}{(m_L + m_R)\left(D_N + \frac{k_x^2}{k^2}\right)}, \tag{39}$$

$$\tan \theta_p^R = -\frac{R_{ps}^{(N)}}{T_{pp}^{(N)}} = -i \frac{k}{k_x} \frac{m_L - m_R}{m_L + m_R}. \tag{40}$$

As it is seen from Eqs. (38) and (40), the θ_s^R and θ_p^R are independent of the number N of sheets and are purely imaginary. The latter means that, in the frame of our approximation, i.e., when $|\gamma| \ll 1$ takes place, there is no rotation of the electric field vector $\vec{E}$ with respect to the initial direction, and for both s and p modes the reflected light is elliptically polarized. This result has been confirmed by our numerical calculations, which indicate that indeed the real parts of θ_s^R and θ_p^R are very small compared to the imaginary parts [see Fig. 2(a), where we have presented only the results for θ_s^R]. However, according to the numerical calculations, the lower panel shows oscillatory behavior of the Kerr rotation (Re θ_s^R), when ω approaches the points $N\beta a = \pi l$. The regions with jump discontinuity ($N - 1$ times in each allowed band) lie precisely on ω, happen on a very short scale, and, at these ω, $\theta_s^R = \pm\pi/2$. Note that, at these values of ω, D_N is $(-1)^l e^{iNk_x a}$ and the reflection coefficients become very small. This type of relation between large Kerr rotation enhancement and a large reduction of the reflection coefficients was experimentally observed in Refs. [6,25]. We would like to stress that, within our assumption $|\gamma| \ll 1$, θ_s^R and θ_p^R are completely independent of the number of the sheets N in a 1D periodic MPC system. The reason is that in this approximation the zeros of $R_{ps}^{(N)}$ and $R_{ss}^{(N)}$ coincide with each other [see Eqs. (29) and (30)]. However, as follows from the transfer matrix calculations, there is a very small separation between the zeros of order of 10^{-7} or $\sim\gamma^2$. Clearly, our analytical approximation is not accurate enough to predict the exact numerical result of order of 10^{-7}, but on the other hand our approximation is good enough to guarantee a sufficient accuracy for fitting all the numerical results presented in

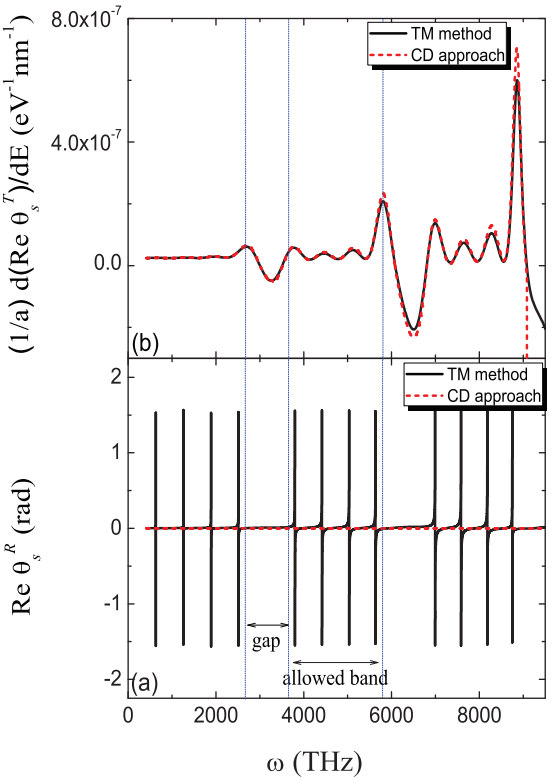

FIG. 2. (Color online) (a) Real part of the Faraday rotation angle θ_s^R and (b) derivative of the real part of θ_s^T versus the frequency ω. The 1D array consists of five magnetoactive sheets with spatial period $a = 529$ nm and $\theta = 1$ rad. The parameters of each MPC are $m_L = 21.32$ nm and $m_R = 0.50$ nm. Dashed lines correspond to theoretical expressions [Eqs. (38)] while the solid curves stand for our numerical calculations via the transfer matrix method.

this paper (see Figs. 2–7). However, these small shifts lead to oscillatory patterns of the θ_s^R. Note that our numerical calculations also show that, in case of disordered systems, the real and imaginary parts of the Kerr rotational angles are of the same order of magnitude. This fact can serve as a precursor of light localization similar to the backscattering peak in the reflected wave [30].

The ratio of the ellipse semi-axes for s modes is determined by the relation ($b_s < a_s$)

$$\frac{b_s}{a_s} = \tanh \operatorname{Im} \theta_s^R = \left| \frac{k_x}{k} \frac{m_L - m_R}{m_L + m_R} \right|, \tag{41}$$

while for p modes it is

$$\frac{b_p}{a_p} = \tanh \operatorname{Im} \theta_p^R = \left| \frac{k}{k_x} \frac{m_L - m_R}{m_L + m_R} \right|. \tag{42}$$

In Ref. [31] the angle of rotation of the polarization and the ellipticity of the light in an external magnetic field are calculated in terms of the density of states and transmission. It was shown that the complex angle of Faraday rotation θ^T in a 1D random layered structure is a self-averaging quantity; i.e., the distribution function of the values of θ^T is logarithmically normal about its geometric mean $\langle \ln \theta^T \rangle$, while its value fluctuates from sample to sample. Moreover, it was shown that θ^T can be expressed through the localization length and density of states for the left- and right-polarized waves [31]. In other words the measurement of the angle of rotation from the frequency gives information on the density of states in random media. The experimental verification of this type of direct connection can be found, for example, in Ref. [16], where a strong enhancement of the Faraday rotation at the edges of the photonic band gap was measured in 1D magnetophotonic crystals. We indeed see in Fig. 2(b) that the derivative of the real part of θ_s^T versus the frequency ω is an oscillating function of ω ($N-1$ times in each allowed band); the amplitudes of the oscillating parts in each allowed band increase with frequency and finally in each forbidden gap $\frac{d\theta_s^T}{d\omega}$ drop markedly. In Ref. [16] it was reported that the Faraday rotation angle in finite MPCs appears to be a nonlinear function of the total thickness of magnetic material in the stack, that can be interpreted as the nonlinear Verdet law. This is in agreement with theoretical expectation discussed in Ref. [31]. One can also come to that conclusion [30] calculating the Faraday rotation angle in a diffusive regime in a three-dimensional disordered slab. Thus, it is clear that in a multilayer system the Faraday rotational angle is not a simple function of the total thickness; the net effect is connected with multiple reflections from each interface, which greatly influences the rotation.

IV. DISORDERED SYSTEMS

In this section we present analytical calculations of the Anderson localization of light propagating through random 1D MPCs system with weak uncorrelated Gaussian disorder. We will demonstrate that, for increasing angle of incidence θ, the localization length of p waves has a tendency to increase, in contrast to what occurs for the localization length of s modes. The latter decreases with increasing angle of incidence and tends to zero at $\theta \to \pi/2$.

In order to achieve this particular goal let us introduce the disorder by considering the magnetoactive sheet parameters m_L and m_R, being random with uniform distribution:

$$m_L = m_{L0} + \delta \mu_L \tag{43}$$

and

$$m_R = m_{R0} + \delta \mu_R, \tag{44}$$

where μ_L and μ_R are zero-mean independent random numbers within the interval $[-0.5,0.5]$. m_{L0} and m_{R0} correspond to the unperturbed MPC parameters while δ stands for the amplitude of the disorder.

In the next standard step we will restrict ourselves to the limit of weak disorder and evaluate the scattering matrix elements of 1D MPC systems, Eqs. (20) and (21), to linear order in the random parameters m_L and m_R. Using the mentioned explicit forms, it can be shown that the transmission, $T_{nm}^{(N)}$, and reflection, $R_{nm}^{(N)}$, amplitudes are given by

$$\begin{aligned} T_{ss}^{(N)} &\approx e^{ik_x(x_N - x_1)} \left(1 + \sum_{l=1}^{N} r_{ss}^{(l)} \right) \\ &= e^{ik_x(x_N - x_1)} \frac{1 + i \sum_{l=1}^{N} y_l}{1 + i \sum_{l=1}^{N} (x_l + y_l)}, \end{aligned} \tag{45}$$

$$T_{sp}^{(N)} \approx e^{ik_x(x_N - x_1)} \sum_{l=1}^{N} r_{ps}^{(l)}. \tag{46}$$

After ensemble-averaging the above partial transmission and reflection coefficients over the random parameters μ_L and μ_R, we obtain, successively,

$$\left\langle \left| T_{ss}^{(N)} \right|^2 \right\rangle = 1 - \frac{Nk^2}{8} \left(1 + \frac{k^2}{2k_x^2} \right) \left[\frac{\delta^2}{6} + N(m_{L0} + m_{R0})^2 \right], \tag{47}$$

$$\left\langle \left| T_{sp}^{(N)} \right|^2 \right\rangle = \left\langle \left| R_{sp}^{(N)} \right|^2 \right\rangle \equiv \frac{Nk^2}{16} \left[\frac{\delta^2}{6} + N(m_{L0} - m_{R0})^2 \right], \tag{48}$$

$$\left\langle \left| R_{ss}^{(N)} \right|^2 \right\rangle = \frac{Nk^4}{16k_x^2} \left[\frac{\delta^2}{6} + N(m_{L0} + m_{R0})^2 \right]. \tag{49}$$

To derive Eqs. (47)–(49) we note that the phases in $T_{nm}^{(N)}$ are irrelevant. In other words, the configuration of sheets is not important for uncorrelated potential in the linear approximation of the perturbation theory, and one might expect to get similar expressions in a quasiperiodic 1D PMC.

It is straightforward to check, based on Eqs. (47)–(49), that the sum of all of them (within $N^2\gamma \ll 1$ approximation) is equal to $1 - N^2\gamma/2$ and the intensity conservation takes place with high accuracy.

A. Localization length

The inverse localization length ξ_j ($j = s,p$) as a function of the system size $L = (N-1)a$ can be defined as

$$\frac{a}{\xi_j} = -\lim_{N \to \infty} \frac{1}{2N} \left\langle \ln \left(\left| T_{jj}^{(N)} \right|^2 + \left| T_{sp}^{(N)} \right|^2 \right) \right\rangle, \tag{50}$$

where the angular brackets $\langle \cdots \rangle$ represent averaging over the disorder.

Now, replacing $\langle \ln(|T_{jj}^{(N)}|^2 + |T_{sp}^{(N)}|^2)\rangle$ by $\ln\langle(|T_{jj}^{(N)}|^2 + |T_{sp}^{(N)}|^2)\rangle$ and assuming that for weak disorder the transmission coefficients are close to 1 and thus the reflection coefficients are close to zero, we can expand the right-hand side of Eq. (50). Next, using the explicit expressions for $T_{nm}^{(N)}$ [see Eqs. (45) and (46)] and after averaging over the random parameters $(m_L)_l$ and $(m_R)_l$ distributed uniformly [Eqs. (43) and (44)] and keeping the terms to order Γ^2, we arrive at the following expression for the inverse of the localization length (for simplicity, we set $m_{0L} = m_{0R} = 0$ below):

$$\frac{a}{\xi_s} = \frac{\delta^2 k^2}{192}\left(1 + \frac{k^2}{k_x^2}\right) \equiv \frac{\pi^2}{48}\left(1 + \frac{1}{\cos^2\theta}\right)\frac{\bar{\delta}^2}{\bar{\lambda}^2}, \tag{51}$$

and

$$\frac{a}{\xi_p} = \frac{\delta^2 k^2}{192}\left(1 + \frac{k_x^2}{k^2}\right) \equiv \frac{\pi^2}{48}(1 + \cos^2\theta)\frac{\bar{\delta}^2}{\bar{\lambda}^2}. \tag{52}$$

In the above expressions we present $k_x = k\cos\theta = \frac{2\pi}{\lambda}\cos\theta$ and introduce the normalized parameters $\bar{\lambda}$ and $\bar{\delta}$ to the spatial period a: $\bar{\lambda} = \frac{\lambda}{a}$, $\bar{\delta} = \frac{\delta}{a}$. These standard results, when $\xi_{s,p} \sim \lambda^2$, are rather general for the light localization length in 1D systems. However, the prefactors are different and are strongly dependent on microscopic details of the random potential (see, e.g., Ref. [2]).

Note that in the absence of magneto-optic activity, i.e., when there is no coupling in between the modes ($\Delta = 0$), Eqs. (51) and (52) reduce to the localization lengths for a 1D uncoupled model, $a\xi_s^{-1}(0) = \frac{\pi^2\bar{\delta}^2}{24\bar{\lambda}^2\cos^2\theta}$ and $a\xi_p^{-1}(0) = \frac{\pi^2\bar{\delta}^2\cos^2\theta}{24\bar{\lambda}^2}$, respectively. It is easy to see that the presence of coupling modes enhances the ξ_s and reduces ξ_p with respect to the values $\xi_s(0)$ and $\xi_p(0)$ obtained when the coupling modes are absent, assuming that the incident angle is not zero. It is worth noticing that, in a random system of isotropic magnetodielectric layers when *characteristic impedance does not change* throughout the system, the inverse localization length grows with the angle of incidence and does not depend on the polarization of the incident wave [32].

Concluding this section, let us note that the localization length for the circularly polarized light can be expressed as

$$\begin{aligned}\frac{a}{\xi_{sp}} &= -\lim_{N\to\infty}\frac{1}{4N}\Big\langle \ln\Big(\big|T_{ss}^{(N)}\big|^2 + \big|T_{sp}^{(N)}\big|^2 \\ &\quad + \big|T_{pp}^{(N)}\big|^2 + \big|T_{ps}^{(N)}\big|^2\Big)\Big\rangle \\ &= \frac{\delta^2}{768k_x^2}\left(k^2 + k_x^2\right)^2 \\ &\equiv \frac{\pi^2}{192}\left(\frac{1+\cos^2\theta}{\cos\theta}\right)^2\frac{\bar{\delta}^2}{\bar{\lambda}^2}.\end{aligned} \tag{53}$$

V. NUMERICAL RESULTS

Up to now, we have presented analytical expressions for the scattering matrix elements and for the localization lengths. The numerical analysis will be useful also to test the theoretical prediction given in the previous sections.

Before we proceed further let us first estimate the parameter γ, using the data from Refs. [11,12] where the magneto-optic response in periodic systems containing ultrathin cobalt magnetic films was discussed. The diagonal and off-diagonal elements of the dielectric tensor are, according to Refs. [11,12], $\epsilon_{xx}^{(\mathrm{Co})} = -12.5035 - i18.4639$ and $\epsilon_{xy}^{(\mathrm{Co})} = -0.7410 + i0.2077$, respectively. The Co layer thicknesses are chosen in the range 0.4–2.0 nm to preserve a perpendicular magnetic anisotropy. The wavelength λ of the laser, where magneto-optic response can be determined with optimum sensitivity, was chosen to be 632.8 nm. Taking into account that the right (left) circular polarization state is given by $\epsilon_{R,L}^{(\mathrm{Co})} = \epsilon_{xx}^{(\mathrm{Co})} \pm i\epsilon_{xy}^{(\mathrm{Co})}$ and assuming the absence of electron damping, we get $|\epsilon_R^{(\mathrm{Co})}| = 12.7$ and $|\epsilon_L^{(\mathrm{Co})}| = 12.3$. Having in mind these numbers, we find $|\gamma| = \frac{4\pi^2\epsilon_R^{(\mathrm{Co})}\epsilon_L^{(\mathrm{Co})}d^2}{\lambda^2} \approx 2.5\times10^{-3}$ ($d = 0.4$ nm) and $|\gamma| \approx 0.06$ ($d = 2$ nm), respectively. As one can see, the parameter γ even in the visible range of light is much less than unity, and thus the characteristic determinant-approach treatment of the photon transport problem in 1D magnetophotonic crystals discussed in our paper is fully justified.

Thus, the above estimation does credit to the characteristic determinant (CD) approach and serves as a good starting point to compare the theoretical results with numerical simulations. First, we present some numerical calculations of the transmission coefficient for s modes, $|T_{ss}^{(N)}|^2 + |T_{sp}^{(N)}|^2 = |T_s^{(N)}|^2$, as well as their corresponding reflection coefficient $|R_{ss}^{(N)}|^2 + |R_{sp}^{(N)}|^2 = |R_s^{(N)}|^2$, of finite one-dimensional arrays with identical magnetoactive sheets (see again Fig. 1). These calculations will be performed via the transfer matrix (TM) method and CD approach for two different values of the magneto-optic parameter Δ. Similarly, a numerical analysis of the coefficients $|T_{pp}^{(N)}|^2 + |T_{ps}^{(N)}|^2 = |T_p^{(N)}|^2$ and $|R_{pp}^{(N)}|^2 + |R_{ps}^{(N)}|^2 = |R_p^{(N)}|^2$ for p modes will be carried out.

In Fig. 3 we show the transmission and reflection coefficients of an array with five identical magnetoactive sheets and spatial period $a = 529$ nm versus the frequency of the incident light ω. The angle of incidence is 1 rad and the parameters of each sheet $m_L = 0.55$ nm and $m_R = 0.50$ nm. In this situation, the magneto-optic parameter $\Delta = 0.05$ nm or, equivalently, four orders of magnitude less than the period a. One notices that both CD and TM methods yield similar results for the reflection coefficients $|R_s^{(N)}|^2$ and $|R_p^{(N)}|^2$ in the allowed bands and gaps for all frequencies ω. The discrepancies between TM and CD can be observed in Figs. 3(a) and 3(c) for the transmission coefficients $|T_s^{(N)}|^2$ and $|T_p^{(N)}|^2$, respectively. Nevertheless, the relative error is roughly 1% for higher frequencies. Moreover, the conservation law for s and p modes, Eq. (35), can be easily checked after simple inspection of Fig. 3. Let us now consider the opposite situation, that is, when the magneto-optic parameter Δ reaches large values. The authors of Ref. [15] used values of $\Delta = 0.2a$ for their numerical calculations of two-dimensional magnetophotonic crystals. In this context, in Fig. 4 we have represented the transmission and reflection coefficients for the same one-dimensional array as in Fig. 3, but now the magnetoactive sheet parameters have been chosen to be $m_L = 113.74$ nm and $m_R = 0.50$ nm. Correspondingly, the magneto-optic parameter is $\Delta = 113.24$ nm, that is, 0.21 times the array period a. In this case we can also appreciate a good agreement between both approaches, which confirms the characteristic determinant as a good theoretical approximation suitable for studying 1D magnetoactive arrays.

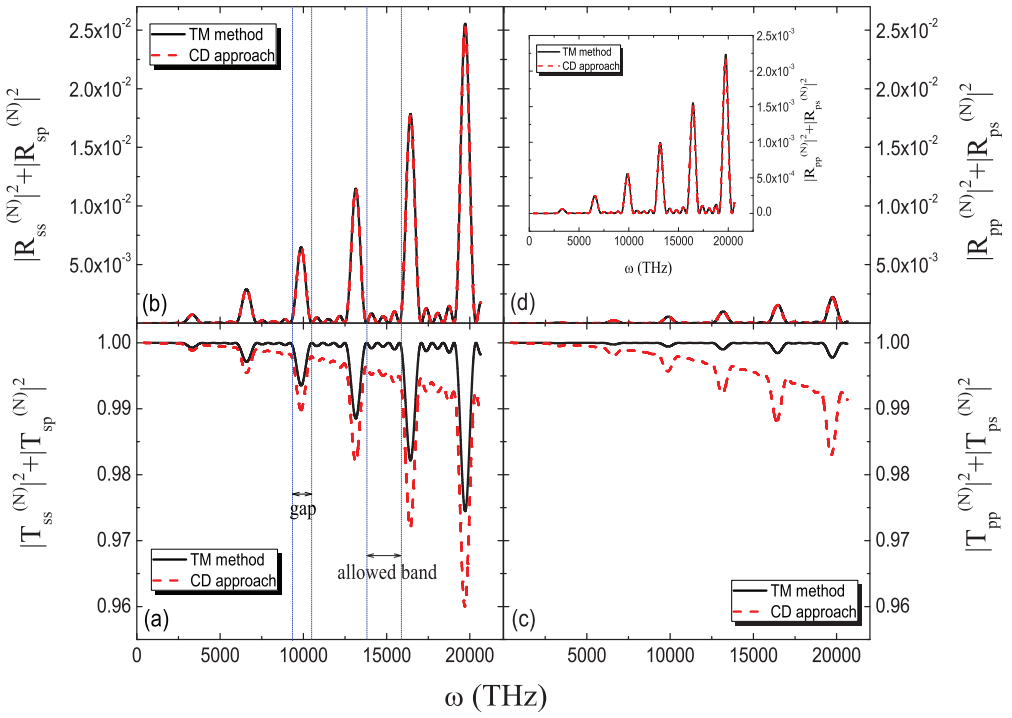

FIG. 3. (Color online) Transmission and reflection coefficients for s modes (left column) and p modes (right column) versus the frequency of the incident light ω. The 1D array consists of five magnetoactive sheets with spatial period $a = 529$ nm and $\theta = 1$ rad. The parameters of each MPC are $m_L = 0.55$ nm and $m_R = 0.50$ nm. Dashed lines correspond to theoretical expressions [Eqs. (27)–(32)].

We have also performed numerical calculations for the localization lengths ξ_s, ξ_p, and ξ_{sp} as a function of the incident wavelength λ and compared them to the theoretical results [see Eqs. (51)–(53)]. Let us now describe our numerical method which was used in order to find the localization length for each polarization mode. For each length L, we calculate the sum

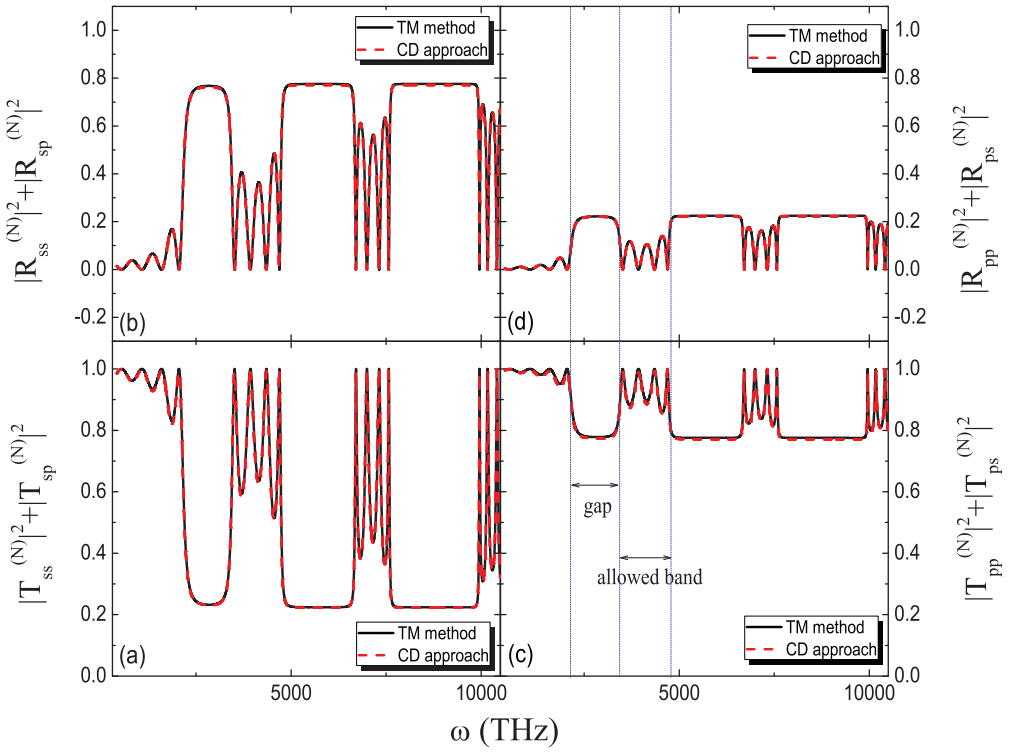

FIG. 4. (Color online) Transmission and reflection coefficients for s modes (left column) and p modes (right column) versus the frequency of the incident light ω. The 1D array is the same as in Fig. 3 but now the magnetoactive sheet parameters have been chosen to be $m_L = 113.74$ nm and $m_R = 0.50$ nm. Dashed lines correspond to theoretical expressions [Eqs. (27)–(32)].

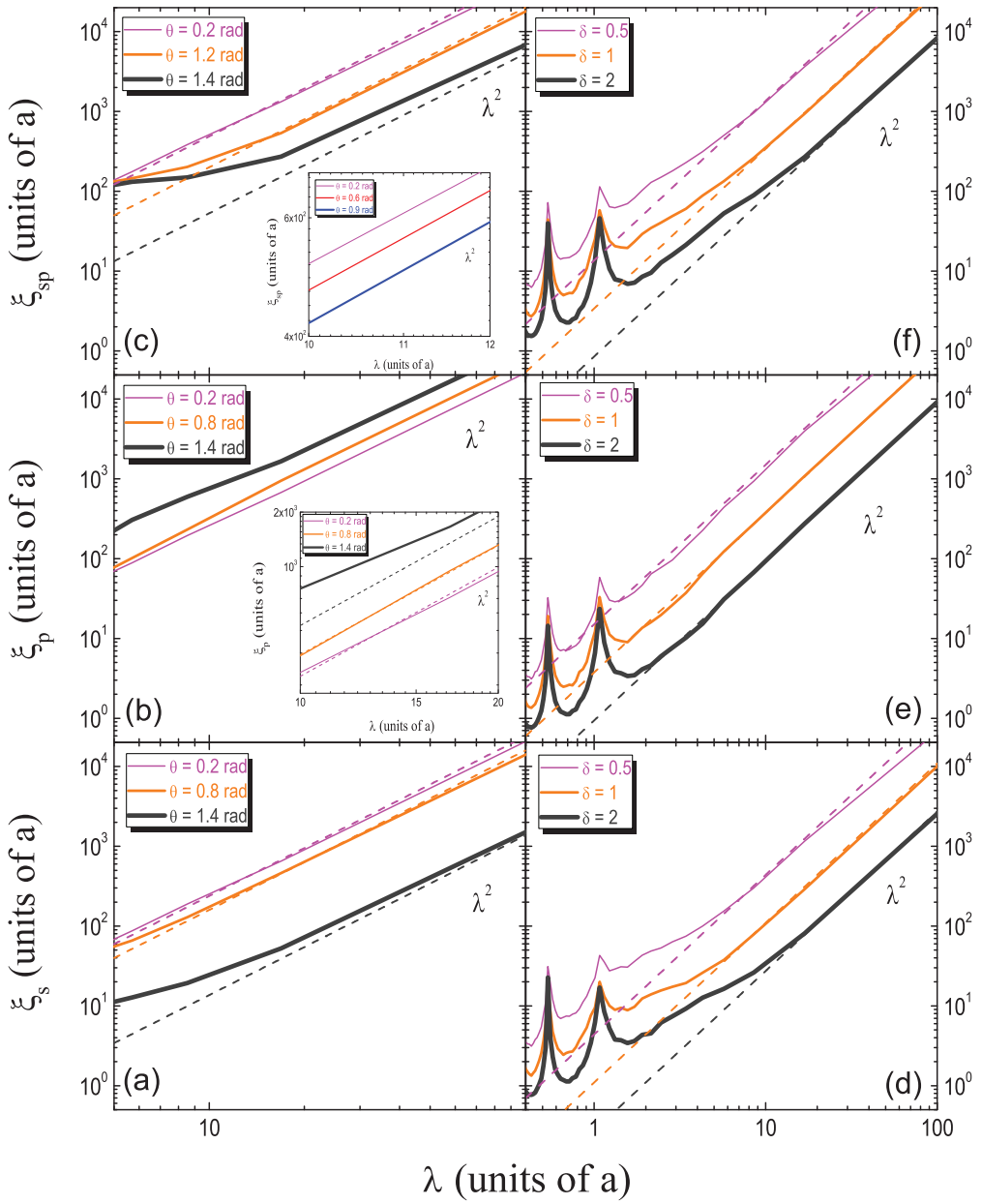

FIG. 5. (Color online) Numerical results for the localization lengths ξ_s, ξ_p, and ξ_{sp} versus the incident wavelength λ as described in the main text. Dashed lines correspond to theoretical expressions [Eqs. (51)–(53)].

$|T_{ss}^{(N)}|^2 + |T_{sp}^{(N)}|^2$ ($|T_{pp}^{(N)}|^2 + |T_{ps}^{(N)}|^2$) via the transfer matrix method and average its logarithm over 800 disorder configurations, using magnetoactive sheet independent random parameters m_L and m_R, defined by Eqs. (43) and (44). Then we numerically obtain the localization length ξ_s (ξ_p) via a linear regression of $\ln(|T_{ss}^{(N)}|^2 + |T_{sp}^{(N)}|^2)$ [$\ln(|T_{ss}^{(N)}|^2 + |T_{sp}^{(N)}|^2)$]. We choose six values of the total length L to perform these linear regressions. The localization lengths ξ_s and ξ_p are then evaluated as a function of the disorder parameter δ, the wavelength of the incident light λ, and the angle of incidence θ, and are compared to our theoretical results, Eqs. (51) and (52), respectively. Similarly, the localization length for circularly polarized light ξ_{sp} is calculated in terms of the sum $|T_{ss}^{(N)}|^2 + |T_{sp}^{(N)}|^2 + |T_{pp}^{(N)}|^2 + |T_{ps}^{(N)}|^2$ [see Eq. (53)]. We remind that in Eqs. (51)–(53) we set $m_{0L} = m_{0R} = 0$, while in our numerical studies the mentioned parameters are not zero. Despite this difference, for all chosen parameters of m_{0L} and m_{0R}, as shown below, the coincidence between our theoretical and the experimental results is very good. The physical reason for this reasonably good agreement is that the disorder parameter δ (in units of the spatial period a) is much larger than m_{0L} and m_{0R}.

Our numerical results for ξ_s, ξ_p, and ξ_{sp} versus the incident wavelength λ are plotted in Fig. 5. The spatial period of all 1D arrays with length L has been chosen to be $a = 529$ nm while the unperturbed parameters of each magnetoactive sheet $m_{L0} = 21.42$ nm and $m_{R0} = 0.50$ nm. In the left column, we have set the disorder parameter $\delta = a$ and have varied the angle of incidence θ. Dashed lines correspond to theoretical expressions [Eqs. (51)–(53)]. It can be noticed that these

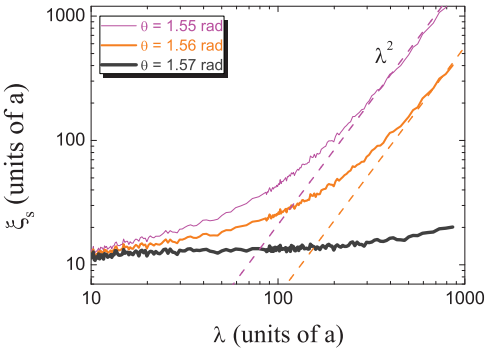

FIG. 6. (Color online) Localization length ξ_s versus the incident wavelength λ at incident angles near $\pi/2$ rad. Dashed lines correspond to the theoretical expression Eq. (51). The 1D array parameters are the same as in Fig. 4(a).

theoretical results fit relatively well the numerical calculations for long wavelengths and a wide range of incident angles θ. The conventional quadratic behavior of ξ with the incident wavelength, $\xi \sim \lambda^2$, is recovered [4,31,33,34], in contrast with recent research which shows a suppression of Anderson localization of light in 1D disordered metamaterials [18–20]. However, the main discrepancies between numerical and theoretical calculations occur at grazing incidences where $\theta \sim \pi/2$ rad, as can be seen in the inset of Fig. 5(b) for ξ_p. Moreover, these p modes are more delocalized at increasing angles θ. We will return to this point later. Having a close look at Fig. 5(c), one observes that the localization length for circularly polarized light ξ_{sp} has a slow dependence on θ up to incident angles of roughly 1 rad, as shown in the corresponding inset. In the right column, the angle of incidence has been fixed to 1 rad and the disorder parameter δ has been changed. Again, a great conformance between numerical and theoretical results can be found at long wavelengths. After a close inspection of Eq. (51) for the localization length ξ_s one can conclude that the s modes become completely localized at grazing incidences, that is, when $\theta \to \pi/2$. In order to obtain the limit of validity of our theoretical results for ξ_s at high angles θ, in Fig. 6 we represent the localization length ξ_s versus the incident wavelength λ for the same parameters as in Fig. 5(a). Dashed lines correspond to the theoretical expression Eq. (51). Notice a good agreement up to angles of incidence of 1.56 rad. It can be also observed that ξ_s is practically independent of λ at incidences near $\pi/2$ rad, a direct consequence of the strong localization at grazing angles.

VI. CONCLUSION

We have provided a complete description of light propagation at an oblique angle of incidence in disordered 1D ultrathin MPCs with an arbitrary number of sheets. We have developed an approach based on the ultrathin film approximation combined with the characteristic determinant method, originally introduced to study the quantum transport of electrons in quasi-one-dimensional disordered systems. In our discussion we included mode conversion and removed the limitations of the normal incident light. Under the condition $\gamma/A \ll 1$, we relate the EMW propagation problem to the Anderson localization of electrons in Q1D systems with two channels. In order to give a more complete analysis of the behavior of EMWs we discuss first the periodic 1D system. We derive exact and closed analytical expressions for all scattering matrix elements which are in excellent agreement with our numerical calculations based on the transfer matrix method. This agreement does credit to the characteristic determinant method and allows to use the determinant method for characterizing the behavior of EMWs in more complex cases, where the exact solution is not available.

We have also studied the magneto-optical Faraday and Kerr effects and calculated analytically the Faraday and Kerr rotational angles for a periodic system. Our formulas predict correctly the main trends of magneto-optic effects in a 1D system. Particularly, we have shown a strong enhancement of the Faraday rotation at the edges of the photonic band gap in 1D magnetophotonic crystals when the interference term is sufficiently large because of forward- and back-scattered electromagnetic waves. We have also demonstrated that the derivative of the real part of the Faraday rotation respect to the energy of incident photons is closely related to the density of states for the left- and right-polarized waves [31]. Equation (37) indicates that the Faraday angle in the finite MPCs appears to be a nonlinear function of the total thickness of magnetic material in the stack, that can be interpreted as the nonlinear Verdet law. This is in agreement with theoretical expectation discussed in Refs. [30,31] and observed in many experimental papers (see, for example, [16,35,36]).

We also derived analytical expressions for photon localization lengths, in a weak disordered regime, for s and p modes and for circular polarized light. Presented analytical expressions for localization lengths are in good agreement with numerical calculations, exact up to order δ^2 (δ being the disorder strength), and valid up to angles of incidence of 1.56 rad. The conventional quadratic behavior of localization length with the incident wavelength λ, i.e., $\xi_{s,p} \sim \lambda^2$, is recovered. However, the prefactors are different and are strongly dependent on microscopic details of the random potential (see, e.g., Ref. [2]). We show that the presence of coupling modes enhances the ξ_s and reduces ξ_p with respect to the values $\xi_s(0)$ and $\xi_p(0)$ obtained when the coupling modes are absent.

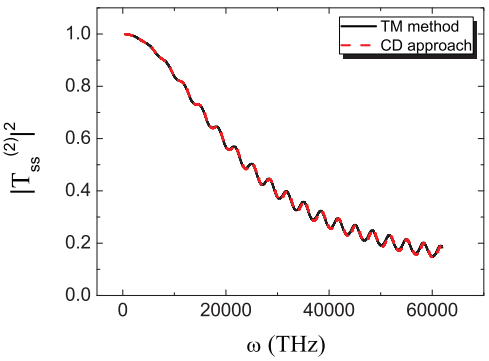

FIG. 7. (Color online) The analytical result for $|T_{ss}^{(2)}|^2$ [Eqs. (A1) and (A4)], based on the transfer matrix and the characteristic determinant methods, respectively. The 1D array consists of two magnetoactive sheets separated by 529 nm and an angle of incidence of 1 rad. The parameters for the first MS are $m_{L1} = 0.55$ nm and $m_{R1} = 0.50$ nm, while for the second one $m_{L2} = 21.64$ nm and $m_{R2} = 0.83$ nm.

ACKNOWLEDGMENT

V.G. acknowledges partial support by FEDER and the Spanish DGI under Project No. FIS2010-16430.

APPENDIX: CHARACTERISTIC DETERMINANT VERSUS TRANSFER MATRIX

For the case of two sheets, multiplying the individual transfer matrices, Eq. (1), by hands yields the following $T_{ss}^{(2)}$:

$$\left(T_{ss}^{(2)}\right)_{\mathrm{TM}} = e^{ik_x a}\frac{\left(1+r_{ss}^{(1)}\right)\left(1+r_{ss}^{(2)}\right)-\left(r_{pp}^{(1)}+\frac{\gamma_1}{A_1}\right)\left(r_{pp}^{(2)}+\frac{\gamma_2}{A_2}\right)e^{2ik_x a}+r_{sp}^{(1)}r_{ps}^{(2)}-r_{sp}^{(1)}r_{ps}^{(2)}e^{2ik_x a}}{1-e^{2ik_x a}\left[2r_{ps}^{(2)}r_{sp}^{(1)}+r_{pp}^{(1)}r_{pp}^{(2)}+r_{ss}^{(1)}r_{ss}^{(2)}\right]+\frac{\gamma_1}{A_1}\frac{\gamma_2}{A_2}e^{4ik_x a}}. \tag{A1}$$

On the other hand, using the explicit expression for $T_{nm}^{(N)}$ [see Eq. (21)], one can rewrite the expression for the amplitude of transmission in terms of a single infinitesimal-thickness magneto-optic active layer reflection amplitude, $r_{nm}^{(l)}$ ($l = 1,2$ and $m,n = s,p$) in the following form:

$$\left(T_{nm}^{(2)}\right)_{\mathrm{CD}} = \frac{e^{ik_x a}}{\det(D_2)}\begin{vmatrix} \delta_{nm} & r_{nm}^{(1)} & r_{nm}^{(2)}e^{ik_x a} \\ 1 & -1 & \left(r_{ss}^{(2)}+\frac{r_{sp}^{(1)}r_{ps}^{(2)}}{r_{ss}^{(1)}}\right)e^{ik_x a} \\ e^{-ik_x a} & \left(r_{ss}^{(1)}+\frac{r_{sp}^{(2)}r_{ps}^{(1)}}{r_{ss}^{(2)}}\right)e^{ik_x a} & -1 \end{vmatrix}, \tag{A2}$$

where $\det(D_2)$, according to Eq. (18), is

$$\det(D_2) = \begin{vmatrix} -1 & \left(r_{ss}^{(2)}+\frac{r_{sp}^{(1)}r_{ps}^{(2)}}{r_{ss}^{(1)}}\right)e^{ik_x a} \\ \left(r_{ss}^{(1)}+\frac{r_{sp}^{(2)}r_{ps}^{(1)}}{r_{ss}^{(2)}}\right)e^{ik_x a} & -1 \end{vmatrix}. \tag{A3}$$

Evaluating the above determinants, we will arrive the approximate expression

$$\left(T_{ss}^{(2)}\right)_{\mathrm{CD}} \approx e^{ik_x a}\frac{\left(1+r_{ss}^{(1)}\right)\left(1+r_{ss}^{(2)}\right)-r_{pp}^{(1)}r_{pp}^{(2)}e^{2ik_x a}+r_{sp}^{(1)}r_{ps}^{(2)}-r_{sp}^{(1)}r_{ps}^{(2)}e^{2ik_x a}}{1-e^{2ik_x a}\left[2r_{ps}^{(2)}r_{sp}^{(1)}+r_{pp}^{(1)}r_{pp}^{(2)}+r_{ss}^{(1)}r_{ss}^{(2)}\right]}. \tag{A4}$$

Figure 7 compares two analytical results for $T_{ss}^{(2)}$. Equation (A1) is based on the transfer matrix method while the analogous expression, Eq. (A4), is calculated using the characteristic determinant method. The very good agreement between transfer matrix and characteristic determinant calculations shows that the determinant approach can properly describe light interference effects due to multiple scattering in the 1D MPCs in the $\frac{\gamma_n}{A_n} \ll 1$ approximation. Accordingly, the determinant method may be explicitly used for a small N to get analytical expression for scattering matrix elements.

[1] *Ultrathin Magnetic Structures IV*, Applications of Nanomagnetism Vol. 4, edited by B. Heinrich and J. A. C. Bland (Springer, Berlin, 2005).

[2] *Optical Properties of Photonic Structures: Interplay of Order and Disorder*, Series in Optics and Optoelectronics, edited by M. F. Limonov and R. M. De La Rue (Taylor and Francis, London, 2012).

[3] P. Yeh, *Optical Waves in Layered Media* (Wiley Interscience, New York, 1988).

[4] P. Sheng, B. White, Z.-Q. Zhang, and G. Papanicolaou, *Scattering and Localization of Classical Waves in Random Media* (World Scientific, Singapore, 1990).

[5] M. Inoue, K. Arai, T. Fujii, and M. Abe, J. Appl. Phys. **83**, 6768 (1998).

[6] M. Inoue, K. Arai, T. Fujii, and M. Abe, J. Appl. Phys. **85**, 5768 (1999).

[7] A. K. Zvezdin and V. I. Belotelov, Eur. Phys. J. B **37**, 479 (2004).

[8] A. Figotin and I. Vitebsky, Phys. Rev. E **63**, 066609 (2001).

[9] A. Figotin, Y. A. Godin, and I. Vitebsky, Phys. Rev. B **57**, 2841 (1998).

[10] K. Busch and S. John, Phys. Rev. Lett. **83**, 967 (1999).

[11] S. Visnovsky, K. Postava, and T. Yamguchi, Opt. Express **9**, 158 (2001).

[12] S. Visnovsky, M. Nyvlt, V. Prosser, R. Lopusnik, R. Urban, J. Ferre, G. Penissard, D. Renard, and R. Krishnan, Phys. Rev. B **52**, 1090 (1995).

[13] T. J. Shepherd and P. J. Roberts, Phys. Rev. E **51**, 5158 (1995).

[14] T. J. Shepherd, P. J. Roberts, and R. Loudon, Phys. Rev. E **55**, 6024 (1997).

[15] A. B. Khanikaev, A. V. Baryshev, M. Inoue, A. B. Granovsky, and A. P. Vinogradov, Phys. Rev. B **72**, 035123 (2005).

[16] A. B. Khanikaev, A. B. Baryshev, P. B. Lim, H. Uchida, M. Inoue, A. G. Zhdanov, A. A. Fedyanin, A. I. Maydykovskiy, and O. A. Aktsipetrov, Phys. Rev. B **78**, 193102 (2008).

[17] S. A. Gredeskul, Y. S. Kivshar, A. A. Asatryan, K. Y. Bliokh, Y. P. Bliokh, V. D. Freilikher, and I. V. Shadrivov, Low Temp. Phys. **38**, 570 (2012).
[18] D. Mogilevtsev, F. A. Pinheiro, R. R. dos Santos, S. B. Cavalcanti and L. E. Oliveira, Phys. Rev. B **82**, 081105(R) (2010).
[19] E. J. Torres-Herrera, F. M. Izrailev, and N. M. Makarov, Europhys. Lett. **98**, 27003 (2012).
[20] O. del Barco and M. Ortuño, Phys. Rev. A **86**, 023846 (2012).
[21] M. Ya. Azbel, Phys. Rev. B **27**, 3901 (1983).
[22] J. B. Pendry, Adv. Phys. **43**, 461 (1994).
[23] V. Gasparian, Phys. Rev. B **77**, 113105 (2008).
[24] V. Gasparian and A. Suzuki, J. Phys.: Condens. Mattter **21**, 405302 (2009).
[25] M. Inoue, A. V. Baryshev, A. B. Khanikaev, E. Dokukin, K. Chung, J. Heo, H. Takagi, H. Uchida, P. B. Lim, and J. Kim, IEICE Trans. Electron. **E91-C**, 1630 (2008).
[26] V. Babikov, *Method of the Phase Functions in Quantum Mechanics* (Nauka, Moskow, 1971).
[27] P. F. Bagwell, J. Phys.: Condens. Matter **2**, 6179 (1990).
[28] V. Gasparian, Sov. Phys. Solid State **31**, 266 (1989) [Fiz. Tverd. Tela **31**, 162 (1989) (in Russian)].
[29] P. Devillard, V. Gasparian, and T. Martin, Phys. Rev. B **78**, 085130 (2008).
[30] V. Gasparian and Z. S. Gevorkian, Phys. Rev. A **87**, 053807 (2013).
[31] A. G. Aronov and V. M. Gasparian, Solid State. Commun. **73**, 61 (1990).
[32] A. I. Ignatov, A. M. Merzlikin, A. P. Vinogradov, and A. A. Lisyansky, Phys. Rev. B **83**, 224205 (2011).
[33] C. Martijn de Sterke and R. C. McPhedran, Phys. Rev. B **47**, 7780 (1993).
[34] T. M. Jordan, J. C. Partridge, and N. W. Roberts, Phys. Rev. B **88**, 041105(R) (2013).
[35] M. Crescimanno, G. Mao, J. H. Andrews, K. D. Singer, E. Baer, A. Hiltner, H. Song, K. Comeau, B. Shakya, A. Bishop, and R. Livingston, J. Opt. Soc. Am. B **29**, 1038 (2012).
[36] G. M. Wysin, V. Chikan, N. Young, and R. K. Dani, J. Phys.: Condens. Matter **25**, 325302 (2013).